# Characterization of *Caenorhabditis elegans* Lectin-Binding Mutants

**Christopher D. Link, Michael A. Silverman, Moira Breen, Kathleen E. Watt and Shale A. Dames**

*Department of Biological Sciences, University of Denver, Denver, Colorado 80208*

Manuscript received January 27, 1992
Accepted for publication April 30, 1992

ABSTRACT

We have identified 45 mutants of *Caenorhabditis elegans* that show ectopic surface binding of the lectins wheat germ agglutinin (WGA) and soybean agglutinin (SBA). These mutations are all recessive and define six genes: *srf-2*, *srf-3*, *srf-4*, *srf-5*, *srf-8* and *srf-9*. Mutations in these genes fall into two phenotypic classes: *srf-2*, *-3*, *-5* mutants are grossly wild-type, except for their lectin-binding phenotype; *srf-4*, *-8*, *-9* mutants have a suite of defects, including uncoordinated movement, abnormal egg laying, and defective copulatory bursae morphogenesis. Characterization of these pleiotropic mutants at the cellular level reveals defects in the migration of the gonadal distal tip cell and in axon morphology. Unexpectedly, the pleiotropic mutations also interact with mutations in the *lin-12* gene, which encodes a putative cell surface receptor involved in the control of cell fate. We propose that the underlying defect in the pleiotropic mutations may be in the general processing or secretion of extracellular proteins.

THE body of the nematode *Caenorhabditis elegans* is surrounded by an acellular, collagenous cuticle (COX, KUSCH and EDGAR 1981; COX, STAPRANS and EDGAR 1981). This cuticle is secreted by the underlying hypodermis, and as such, is representative of the developmental and biochemical state of this tissue. The hypodermis of *C. elegans* consists of a single layer of cells, derived from 78 embryonic cells (SULSTON *et al.* 1983). As pointed out by HEDGECOCK *et al.* (1987), the hypodermis not only secretes the cuticle, but is also intimately involved (directly or indirectly) in guiding the attachment and migration of underlying muscle, neuronal, and gonadal cells.

We have previously shown that the surface of the cuticle is specifically modified at the hermaphrodite vulva and the male copulatory bursa by demonstrating that these regions specifically bind the lectin wheat germ agglutinin (WGA) (LINK, EHRENFELS and WOOD 1988). It is not known how (or why) the hypodermis restricts lectin-binding components to specific regions of the cuticle. Cuticle surface binding of lectins has been observed in other free-living (ZUCKERMAN, KAHANE and HIMMELHOCH 1979) and parasitic (RUDIN 1990) nematodes, and in some instances, specific glycoproteins have been implicated (MAIZELS *et al.* 1989; SELKIRK *et al.* 1990). Little work has been done on glycosylation or glycoproteins in *C. elegans*; the cuticle surface component(s) bound by WGA have not been identified. [The carbohydrate bound by WGA is presumably not sialic acid, as this carbohydrate has recently been shown to be absent in *C. elegans* (BACIC, KAHANE and ZUCKERMAN 1990).]

By identifying mutants with altered lectin-binding phenotypes, we have sought to identify genes involved in hypodermal function. We have sought mutants that show ectopic lectin binding, as opposed to absence of lectin binding, because these mutants are technically much easier to identify in large-scale screens. (Because surface lectin binding is restricted to small regions of the adult wild-type animal, mutants missing this lectin binding are difficult to identify in a dissecting microscope screen.) There is a precedent for ectopic lectin-binding mutants: in *lin-22* mutants, which show alteration of hypodermal cell fate such that anterior cells assume the fate of more posterior cells (HORVITZ *et al.* 1983), male animals show strong ectopic binding of WGA (LINK, EHRENFELS and WOOD 1988).

As described below, we have recovered 45 mutant strains that define six genes that can be mutated to produce an ectopic lectin binding phenotype. Mutations in three of these genes have extensive pleiotropic effects, suggesting that these genes play multiple roles in the development of *C. elegans*.

## MATERIALS AND METHODS

**Strains and general methods:** All strains used in this work were derived from *Caenorhabditis elegans* var. Bristol strain N2. Culturing, handling, and genetic manipulation were as described by BRENNER (1974); all experiments were performed at 20° unless noted otherwise. Nomenclature follows the guidelines of HORVITZ *et al.* (1979). Neuronal designations are those used by WHITES *et al* (1986). The following genes and alleles were used:

Linkage group (LG) I: *dpy-5(e61)*, *srf-2(yj262)*;
LG II: *bli-2(e768)*;
LG III: *unc-32(e189)*, *dpy-17(e164)*, *lin-12(n302, n379, n676 n930, n676 n904am)*, *daf-2(e1370)*;
LG IV: *unc-5(e53)*, *srf-3(yj10)*;
LG V: *dpy-11(e224)*, *unc-51(e369)*, *him-5(e1490, e1467)*,

*rol-9(sc148), unc-76(e911), sma-1(e30), unc-23(e25), unc-68(e540), unc-42(e220), her-1(n695, y101), dpy-21(e428), par-4(it33), fog-2(q71);*

LG X: *lon-2(e678), unc-9(e101), lin-15(n765).*

(New alleles generated in this work are described in Table 2.)

*srf-2* and *srf-3* have been described by POLITZ *et al.* (1990); *lin-12* by GREENWALD, STERNBERG and HORVITZ (1983); *daf-2* by RIDDLE, SWANSON and ALBERT (1981); *him-5* by HODGKIN, HORVITZ and BRENNER (1979); *fog-2* by SCHEDL and KIMBLE (1988); *her-1 (n695)* by TRENT, WOOD and HORVITZ (1988); *dpy-21(e428)* by HODGKIN and BRENNER (1977); and *par-4* by KEMPHUES *et al.* (1988). *rol-9 (sc148)* was isolated by R. S. EDGAR (personal communication) and *her-1(y101)* by A. VILLENEUVE and B. MEYER (personal communication). All other mutants were described by BRENNER (1974).

The following genetic rearrangements were also used: translocations eT1 (ROSENBLUTH and BAILLIE 1981) and nT1 (SANFORD, GOLOMB and RIDDLE 1983); and genetic deficiencies *sDf20*, *sDf29* (ROSENBLUTH, CUDDEFORD and BAILLIE 1985), *sDf35* (MCKIM, HESHL and BAILLIE 1988), *ctDf1* (MANSER and WOOD 1990), *ozDf1*, *oz Df2* (T. SCHEDL, personal communication), and *yDf4* (B. MEYER, personal communication).

**Screening for lectin-binding mutants:** Animals were mutagenized by incubation in 0.5% or 0.25% ethyl methyl sulfonate (EMS) as described by BRENNER (1974). Mutagenized fourth larval stage (L4) or young adult animals were transferred to large (100 × 15 mm) NGM plates seeded with *Escherichia coli*, five animals per plate. These animals were allowed to propagate for two generations, at 20° (7–8 days), at which point these plates contained roughly 5000 adult $F_2$ animals. The $F_2$ animals were stained for surface lectin binding as follows (all incubations at room temperature). Animals were rinsed from plates and washed three times in M9 buffer by centrifugation in a low-speed centrifuge, then incubated for 90 min in 50 μg/ml biotinylated WGA (Vector Labs Inc., 5 mg/ml stock diluted 1:100 in M9 buffer). Animals were then washed 2 × in M9 and incubated for 90 min in 50 μg/ml avidin-horseradish peroxidase (Vector Labs Inc., 5 mg/ml stock diluted 1:100 in M9 buffer). Animals were again washed two times in M9 buffer, then resuspended in 200 μg/ml of the chromogen 3-amino-9-ethylcarbazole (4 mg/ml stock solution in *N*-dimethyl formamide, diluted 1:20 in 0.05 M citrate buffer, pH 5.0). Staining of animals was initiated by addition of $H_2O_2$ to a final concentration of 0.01%. After five to ten minutes, chromogenic development was quenched by washing animals in M9 buffer. This treatment results in the WGA-binding portion of animals staining red-brown. (Although most animals readily survive this staining protocol, strongly staining animals suffer significant cuticle damage, presumably from localized oxidative damage resulting from the activity of the bound horseradish peroxidase. Although this cuticle damage is usually fatal, the eggs of gravid hermaphrodites remain viable, so progeny are readily recovered from strongly staining candidate mutants.)

After staining, animals were transferred to large agar plates, and those showing ectopic staining were identified using a dissecting microscope (outfitted with a thin piece of white paper over the transillumination source to whiten background illumination). This method allows the rapid screening of large populations of mutagenized animals. The progeny of candidate mutants were retested by incubation in fluorescently labeled WGA [WGA-fluorescein isothiocyanate (FITC)] and subsequent observation by epifluorescence microscopy as previously described (LINK, EHRENFELS and WOOD 1988). The seven screens used to generate the alleles described in this work are summarized in Table 1. To assure independence of the recovered mutants, only one mutant was retained from each independently processed population of animals. Therefore, our calculated frequency of approximately one mutant/10,000 $F_2$ animals screened significantly underestimates the actual mutation frequency for this phenotypic class.

**TABLE 1**

**Summary of mutagenesis experiments**

| Mutagenesis | [EMS] (%) | Parental strain | No. of $F_2$ screened | Alleles recovered |
|---|---|---|---|---|
| A | 0.5 | *n695* | 33,000 | *ct104-ct109* |
| B | 0.5 | wt | 26,000 | *ct110, 111, 112* |
| C | 0.5 | *n695* | 50,000 | *ct113-ct118* |
| D | 0.25 | *y101* | 18,000 | *dvl* |
| E | 0.25 | *y101* | 30,000 | *dv2, 3, 4, 5* |
| F | 0.25 | *y101* | 140,000 | *dv7-dv18* |
| G | 0.25 | *y101* | 180,000 | *dv20-dv40* |

Mutagenesis and screening performed as described in MATERIALS AND METHODS. wt = wild type.

**Complementation analysis:** All mutants that showed consistent ectopic WGA binding [thus having the Surface (Srf) phenotype] were tested for their heterozygous phenotype by mating these mutants with wild-type males and examining the resulting cross-progeny animals by staining with WGA-FITC. [Because most mutants were isolated in an *n695* or *y101* background, cross-progeny could be easily identified as non-egg-laying defective (nonEgl) hermaphrodites.] All alleles were recessive in this test. Initial isolates were outcrossed to *him-5(el490)*, and *him-5* double mutants were recovered. Alleles were tested for complementation either by mating *him-5; mutant 1*($m_1$) males to *n695 (or y101)*; $m_2$ hermaphrodites, and scoring the resulting nonEgl cross-progeny, or by mating $m_1$/+ males to *dpy-17(e164)*; $m_2$ hermaphrodites and scoring the nonDpy cross-progeny, one-half of which will be mutant if noncomplementation is observed. In this manner the 45 mutants tested were assigned to six complementation groups.

**Mapping of representative alleles:** *dv25*, one of 27 alleles in the largest complementation group, was mapped to LGI using the mapping strains *dpy-5(e61)I; bli-2(e768)II; unc-32(e189)III;* and *unc-5(e53)IV; dpy-11(e224)V; lon-2(e678)X. him-5; dv25* males were mated to mapping strain hermaphrodites, and phenotypically wild-type cross-progeny were recovered. The self-progeny of these animals were then screened for WGA binding to recover *dv25* homozygous animals. If *dv25* is unlinked to a given marker gene, then ⅔ of these *dv25* homozygous (but otherwise phenotypically wild type) animals should be heterozygous for this marker. This prediction held true for all markers except *dpy-5*, where only 1/9 *dv25* homozygous animals segregated *dpy-5* self-progeny, indicating linkage to LGI. Since the previously identified *srf-2* gene also maps to this linkage group (POLITZ *et al.* 1990), the reference allele, *srf-2(yj262)*, was tested for WGA binding and for complementation with *dv25* and other alleles of this complementation group. *srf-2(yj262)* was found to bind WGA and failed to complement all of the *dv25* complementation group alleles tested. Thus, *dv25* and the other members of this complementation group are alleles of *srf-2*.

*ct107* was the sole member of its complementation group.

Unlike the other mutants described in this paper, *ct107* shows somewhat weak WGA staining. However, this mutant does have a strong, highly penetrant SBA-binding phenotype. *ct107* was mapped to LG IV with the mapping protocol described above, using SBA binding to identify *ct107* homozygotes. Since the previously identified *srf-3* gene also maps to this linkage group (POLITZ *et al.* 1990), the reference allele *srf-3(yj10)* was tested for SBA binding and complementation of *ct107*. *srf-3(yj10)* also binds SBA and fails to complement *ct107*. Thus, *ct107* is an allele of *srf-3*.

*ct115* was assigned to a six-member complementation group that appeared *X*-linked: when wild-type males were mated to *ct115* homozygous hermaphrodites, cross progeny males, but not hermaphrodites, showed the *ct115* lectin-binding phenotype. By three-factor mapping, *ct115* lies between *unc-9* and *lin-15*: from *unc-9* + *lin-15*/+ *ct115* + heterozygotes, 1/11 Unc nonLin and 10/11 Lin nonUnc recombinants were heterozygous for *ct115*. From *unc-9* *ct115*/+ + heterozygotes, 70/72 Unc segregants retain *ct115*, placing *ct115* approximately 1.4 map units (0.2–4.8 map units at a 95% confidence level) to the right of *unc-9* on the genetic map. The *ct115* complementation group defines a novel genetic locus, designated *srf-5*.

*ct109* is one of eight mutations that fail to complement and also have very similar pleiotropic effects. All members of this complementation group are uncoordinated (Unc) and have protruding vulvae (P-vul) and abnormal male bursae (Mab), in addition to their lectin-binding phenotype. Initial outcrossing experiments suggested that *ct109* was linked to *him-5 V*. The following three-factor cross indicated that ct109 was closely linked to *unc-51*: from *dpy-11* + *unc-51*/+ *ct109* + heterozygotes, 64/64 Dpy-nonUnc recombinants were heterozygous for *ct109*. The following four factor cross was performed to order *ct109* with respect to *unc-51*: from *ct109* + + *rol-9*/+ *unc-51* *fog-2* + heterozygotes, 33 Rol nonSrf recombinants were identified. Of these recombinants, 8/33 were heterozygous for *unc-51* and *fog-2*, 15/33 were heterozygous for *unc-51*, but not *fog-2*, and 10/33 were heterozygous for neither *unc-51* nor *fog-2*. By extrapolation from the previous estimate of 0.65 map unit between *unc-51* and *fog-2* (T. SCHEDL, personal communication), *ct109* lies approximately 0.4 map unit to the left of *unc-51* on the genetic map. *ct109* was not complemented by *ozDf1* or *ozDf2*, two deficiencies that had previously been shown to include *unc-51* and *fog-2* (T. SCHEDL, personal communication), as demonstrated by the following crosses: when *srf-4*/+ males were mated to *ozDf1/unc-76* *rol-9* or *ozDf2/dpy21* *par-4* hermaphrodites, half of the cross-progeny males had an Unc Mab Srf phenotype. The *ct109* complementation group defines a new gene designated *srf-4*.

*dv38* has pleiotropic effects very similar to *ct109*, but complements this and other *srf-4* alleles. In outcrossing experiments, *dv38* also appeared linked to *him-5*. The following three-factor cross demonstrates that *dv38* maps between *unc-23* and *sma-1* (clearly away from *srf-4*): from *unc-23* + *sma-1*/+ *dv38* + heterozygotes, 11/15 Unc nonSma recombinants were heterozygous for *dv38*, and 2/11 Sma nonUnc recombinants were heterozygous for *dv38*. Deficiency mapping was used to confirm this map position. *dv38* is complemented by *sDf20*, *sDf35* and *ctDf1* as demonstrated by the following crosses: when *dpy-11* *dv38*/+ + males were mated to *eT1/sDf20* hermaphrodites, all Dpy cross-progeny were nonSrf; when *unc23* *dv38*/+ + males were mated to *eT1/sDf35*, all Unc cross-progeny were nonSrf; and when *dv38* *sma-1*/+ males were mated to *nT1* *unc(n754)/ctDf1* hermaphrodites, all Sma cross-progeny were nonSrf. These results place *dv38* in an interval to the left of *sma-1*, between the right endpoint of *sDf35* and the left endpoint of *ctDf1*. The following two-factor cross also places *dv38* left of *sma-1*, approximately 2.65 map units from *dpy-11*: from *dpy-11* *dv38*/+ + heterozygotes, 24/452 Dpy progeny fail to segregate *dv38*. *dv38* defines a new gene, designated *srf-8*.

The noncomplementing mutations *dv4* and *dv16* have the same pleiotropic effects as *srf-4* and *srf-8* alleles, but complement alleles of these genes. Outcrossing experiments again indicated that *dv4* was linked to *him-5*. The following three-factor cross indicated that *dv4* mapped between *dpy-11* and *unc42*: from *dpy-11* + *unc-42*/+ *dv4* + heterozygotes, 7/13 Dpy nonUnc recombinants were heterozygous for *dv4*, while 2/6 Unc nonDpy were heterozygous for *dv4*. Deficiency mapping confirmed that *dv4* mapped to a different interval than *srf-8*. *dv4* was complemented by *sDf20* and *sDf29*, but not *mDf3*, as demonstrated by the following crosses: *dpy-11* *dv4*/+ + males mated to *eT1/sDf20* hermaphrodites produced Dpy outcross that were nonSrf; *dv4* *unc-42*/+ + males mated to *eT1/sDf29* hermaphrodites produced Unc cross-progeny that were nonSrf; but *dv4* *unc42*/+ + males mated to *mDf3/unc-23* *sma-1* hermaphrodites produced Unc(-42) cross-progeny that were also Srf. These experiments localize *dv4* to an interval between the left endpoints of *mDf3* and *sDf29*, near *rol-3*. The following two-factor cross places *dv4* approximately 1.9 map units to the right of *dpy-11*: from *dpy-11* *dv4*/+ + heterozygotes, 13/339 Dpy segregants were nonSrf. *dv4* and *dv16* define a new gene, designated *srf-9*.

The approximate map position of the genes described in this paper are shown in Figure 1.

**Construction of *srf-9 srf-8 srf-4* triple mutant:** First, a *srf-9 srf-8* double mutant was constructed by screening *srf-9* + *unc-42* +/+ *unc-23* + *srf-8* heterozygotes for Srf nonUnc(-42 or -23) recombinants. One recombinant was identified that resulted from a recombinantion event between *unc-23* and *unc-42*, resulting in a *srf-9* + + *srf-8* chromosome. A homozygous *srf-9 srf-8* strain was established and its genotype was verified by complementation testing. A *srf-9 srf-8 unc-51* strain was then constructed by identifying Unc(-51) Srf recombinants from *srf-9 srf-8* +/+ + *unc-51* heterozygotes. *srf-9 srf-8 unc-51*/+ + + males were mated to *sma-1 srf-4* hermaphrodites and *srf-9 srf-8* + + *unc-51*/+ + *sma-1* *srf-4* + heterozygotes were recovered. Srf nonSma nonUnc recombinants were recovered from these heterozygotes, thus establishing a *srf-9 srf-8 srf-4* triple mutant strain. The genotype of this strain was also verified by complementation testing.

**Construction of transgenic strains:** Strains containing the chimeric *mec-7/lacZ* transgene were derived from strain JN640, in which an extrachromosomal array (*evEx1*) containing *mec-7/lacZ* and *rol-6* transgenes has been integrated into LGI, generating *jeIn1 I* (M. HAMELIN, personal communication). This strain has a dominant Roller (Rol) phenotype; genetic constructs containing the transgenes can be identified by virtue of their Rol phenotype. *jeIn1*/+ males were mated to *srf* hermaphrodites, and Rol nonSrf cross-progeny (*jeIn1*/+; *srf*/+) were identified. Self-progeny of these animals were picked, and Srf segregants from Rol homozygous clones were recovered.

**Immunocytochemistry:** γ-Amino butyric acid-containing (GABAnergic) neurons were visualized using a modification of the anti-serotonin immunocytochemical protocol described by DESAI *et al.* (1988) (S. MCINTIRE and L. BLOOM, personal communication). Animals were fixed in 4% paraformaldehyde, 1% gluteraldehyde in phosphate-buffered saline (PBS): 50 mM $Na_2HPO_4$, 140 mM NaCl, pH 7.2) for 16–18 hr at 4°. After washing three times in PBS, animals were incubated for 48 hr at 37° in 5% β-mercaptoethanol,

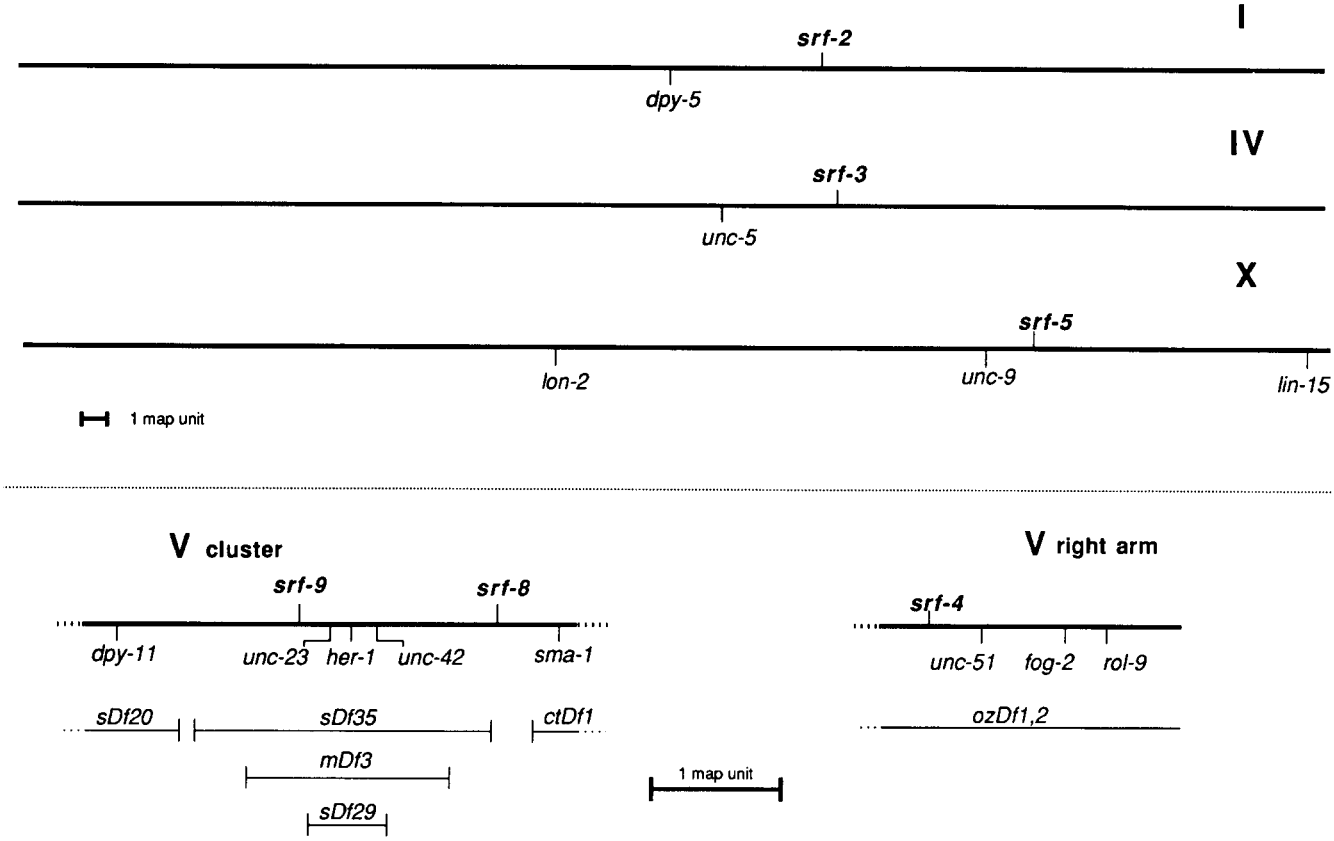


FIGURE 1.—Genetic map positions of *srf* genes. Approximate genetic map positions of the *srf* genes relative to marker genes were determined as described in MATERIALS AND METHODS, except for *srf-2* and *srf-3*, whose positions are based on the data of POLITZ *et al.* (1990).

1% Triton X-100, and 125 mM Tris, pH 7.4, with gentle agitation. Animals were then digested with 2 mg/ml collagenase (Sigma type IV, 460 units/mg) in 100 mM Tris-HCl, pH 7.5, 1 mM $CaCl_2$ by agitating vigorously at 37° for 1–2 hr. After washing three times in PBS, animals were incubated in rabbit anti-GABA serum (Sigma) diluted 1:100 in incubation buffer [1% bovine serum albumin (BSA), 0.5% Triton X-100, 0.05% sodium azide, 1 mM EDTA in PBS] for 24 hr at room temperature. Animals were then washed four times in wash buffer (0.1% BSA, 0.5% Triton X-100, 0.05% sodium azide, 1 mM EDTA in PBS) for a total of 2.5 hr at room temperature before being incubated in FITC-conjugated secondary antibody (goat anti-rabbit, U.S. Biochemical, 1:100 dilution in incubation buffer) for 3 hr at room temperature. Animals were then washed 4X in wash buffer (including one 10-min wash in wash buffer containing 10 μg/ml Hoechst 33258) before being mounted on agarose slabs (50 mM Tris-Cl, pH 9.5, 5 mM $MgCl_2$, 2% agarose).

The ALM neurons were stained with monoclonal antibody 6-11B-1 using the whole mount squash protocol of SIDDIQUI (1990), without modification. Muscles were stained using the actin probe Bodipy-phallacidin (Molecular Probes, Inc.). Animals were fixed in 4% paraformaldehyde (in PBS) at 4° for at least 24 hr, then permeablized using the reduction/oxidation protocol of FINNEY and RUVKIN (1990). Fixed and permeablized animals were stained for at least 1 hr at room temperature in 200 μl of antibody binding buffer containing 1 unit of Bodipy-phallacidin.

β-Galactosidase-expressing neurons were visualized by a protocol derived from published procedures (FIRE 1986). Animals containing the *jeIn1* transgene were grown for at least 2 days at 25°, then washed free of bacteria and resuspended in PBS. The animals were then fixed for 15 min in 2.5% glutaraldehyde at room temperature. After washing in $H_2O$, the animals were lyophilized by placing a 10-μl drop on a microscope slide and drying in a Savant speed concentrator for 15 min. After dipping slides in acetone (−20°) for 3 min, β-galactosidase activity was detected by placing a 50–100-μl drop of X-Gal staining solution (FIRE 1986) on the slides and incubating at 37° for 24 hr.

## RESULTS

**Identification of lectin-binding mutants:** We sought to devise a screen that could identify, and recover self-progeny from, mutants that ectopically bound WGA, even if this ectopic binding was restricted to male animals (as is the case, for example, with *lin-22* mutants). Most of our screens were therefore done by mutagenizing the gain-of-function *her-1* alleles *n695* or *y101*. These alleles variably transform *XX* (normally hermaphrodite) animals into intersexual animals that are usually self-fertile but have masculinized somatic tissues. In a reconstruction experiment, approximately 20% of self-fertile *lin-22(n372); her-1(y101) XX* animals were sufficiently transformed to show the ectopic surface binding of WGA characteristic of *lin-22(n372)* males.

Mutagenized animals were screened for ectopic surface binding of the lectin WGA using a biotinylated-WGA/avidin-horseradish peroxidase staining protocol (described in detail in MATERIALS AND METHODS).

**TABLE 2**

**Summary of complementation analysis**

| Gene | Alleles identified |
|---|---|
| *srf-2 I* | *ct104, 105 110, 112, 116, 117*<br>*dv1, 2, 3, 6, 9, 10, 12, 13, 14, 15, 19, 21, 22, 23, 24, 25, 26, 27, 31, 34, 37* |
| *srf-3 IV* | *ct107* |
| *srf-4 V* | *ct109, 11, 113*<br>*dv11, 20, 35, 36, 39* |
| *srf-5 X* | *ct114, 115*<br>*dv18, 28, 32, 40* |
| *srf-8 V* | *dv38* |
| *srf-9 V* | *dv4, dv16* |

Complementation analysis, genetic mapping and gene assignments are described in MATERIALS AND METHODS.

Candidate mutants were retested by staining with WGA-FITC and by examining with epifluoresence microscopy. Mutations that resulted in consistent WGA-binding phenotypes were assigned to complementation groups by complementation analysis, and representative alleles of each complementation group were positioned on the genetic map. The 45 mutants analyzed were all recessive and identified six genes: *srf-2*, *-3*, *-4*, *-5*, *-8* and *-9* (see Tables 1 and 2, and Figure 1). Alleles of two of these genes, *srf-2* and *srf-3*, have previously been recovered in a screen using adult-specific anti-cuticle antisera (POLITZ *et al.* 1990). Representative alleles of the newly identified genes, *srf-4*, *-5*, *-8* and *-9*, were outcrossed ten times before phenotypic analysis.

The ectopic WGA-binding pattern of representative alleles of the six *srf* genes are shown in Figure 2. All of these alleles have highly penetrant ectopic lectin-binding phenotypes in both males and hermaphrodites; males for all alleles showed more intensive posterior staining than hermaphrodites. For all alleles, there was some variability in the expressivity of the staining phenotype. No allele could be distinguished solely on the basis of its staining phenotype, with the exception of *srf-3*. Both *srf-3* alleles (*yj10* and *ct107*) had weaker staining in both hermaphrodites and males than the other *srf* alleles, characteristically staining only in the area surrounding the vulva in hermaphrodites and the posterior in males (see Figure 2C). The observation that both sexes stain suggests that the ectopic WGA binding is not the result of the type of changes in cell fate observed in *lin-22* mutants. Consistent with this view, the adult lateral alae (a marker for hypodermal cell fate) of *srf* mutants are normal, as judged by differential interference contrast (DIC) microscopy. These mutants also show ectopic binding of the lectin soybean agglutinin (SBA), but not concanavalin A (data not shown).

**Light microscope observations:** Although all of the *srf* mutants we have isolated show similar patterns of lectin binding, these mutants could easily be divided into two classes based on their phenotypes under the dissecting microscope. Alleles of *srf-2*, *srf-3* and *srf-5* appeared grossly wild-type in morphology and movement, and males carrying these mutations mated well. Conversely, *srf-4*, *srf-8* and *srf-9* mutants showed uncoordinated movement, a distinctive body morphology including protruding vulvae, and male infertility. (These phenotypes were all recessive and highly penetrant.) Furthermore, these pleiotropic mutants showed a progressive egg-laying defect (see Figure 3) and produced dauer larvae that were sodium dodecyl sulfate (SDS)-sensitive. (These phenotypes are summarized in Table 3.) The pleiotropic mutants were examined in more detail to better understand the basis of the multiple phenotypes. One question we sought to answer was whether an altered cuticle could account for all the observed defects. As described below, the many abnormalities observed in the pleiotropic mutants suggest a more pervasive underlying defect, possibly one in hypodermal function.

To investigate whether the egg-laying defect of the pleiotropic *srf* mutants has a neuronal or muscular origin, we examined the response of the *srf* mutants to exogenous serotonin or imipramine (a serotonin agonist). The vulval muscles are innervated by the serotonergic HSN neurons, and exogenous serotonin or imipramine will stimulate egg-laying in wild-type *C. elegans* (TRENT, TSUNG and HORVITZ 1983). As argued by these authors, an egg-laying defective mutant with nonfunctional vulval muscles would not respond to either serotonin or imipramine, while a mutant with nonfunctional HSN neurons would respond to serotonin (by direct stimulation of the vulval muscles), but not imipramine, which acts by blocking neuronal re-uptake of serotonin. We found that all the pleiotropic *srf* mutants had reduced sensitivity to both serotonin and imipramine (see Table 4). Although this result is consistent with a muscular basis for the egg-laying defect in these mutants, other interpretations are possible (see DISCUSSION).

Male animals containing *srf-4*, *srf-8* or *srf-9* mutations were examined by DIC microscopy. All these mutants had abnormal copulatory bursae characterized by a reduced fan and a swollen bursa. The sensory rays were normal in number but generally shortened. In addition, the copulatory spicules were commonly crumpled or malformed (see Figure 4, A and B).

DIC microscopy also revealed that *srf-4*, *srf-8* and *srf-9* hermaphrodites have variably abnormal gonad morphology. The wild-type adult hermaphrodite gonad is a bilobed structure that is derived from a 4-cell primordium located ventrally in the midbody of first stage larvae (KIMBLE and HIRSH 1979). Extension of this primordium and proper reflection of the grow-

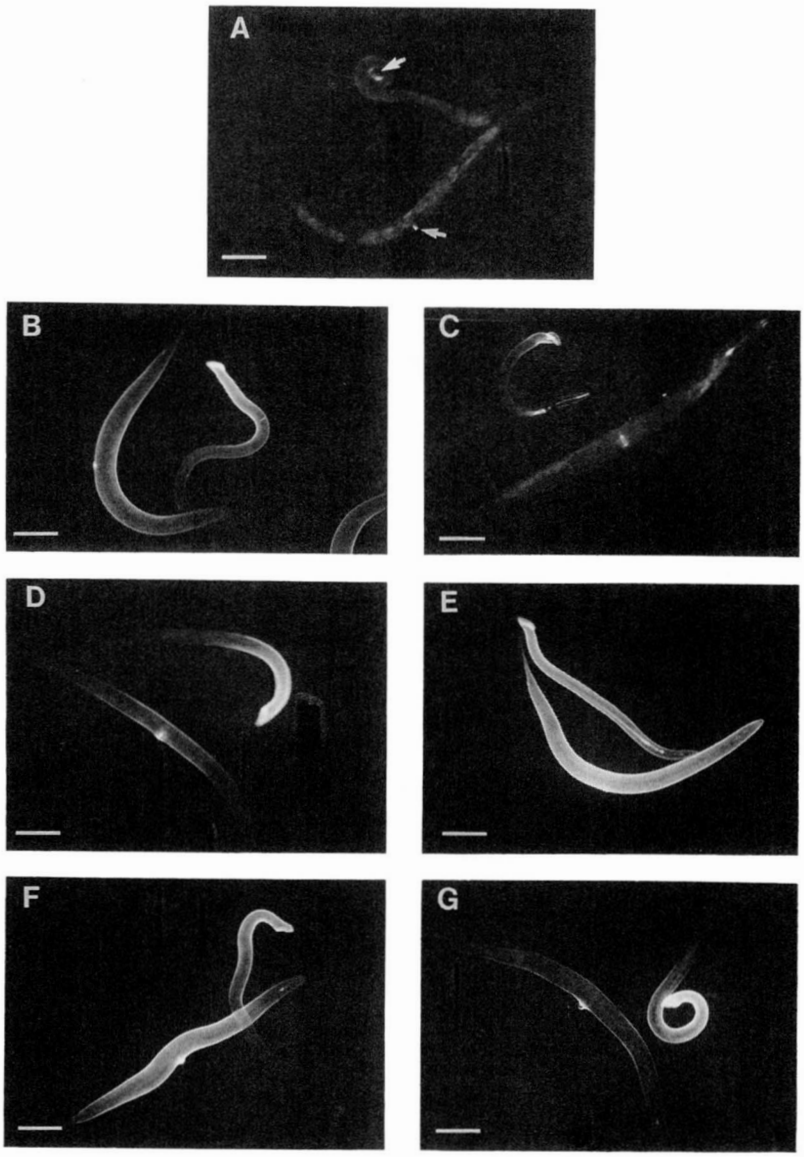


FIGURE 2.—Surface binding of WGA by wild-type and mutant animals. Live male and hermaphrodite animals of each genotype were stained with WGA-FITC as described (LINK, EHRENFELS and WOOD 1988). A, Wild-type. WGA binding is restricted to the male tail and the hermaphrodite vulva (arrows). Faint whole-animal staining results from endogenous autofluorescence, as demonstrated by control observations of unstained animals. B, *srf-2(ct104)*. C, *srf-3(ct107)*. Surface WGA binding in these animals is reduced relative to other *srf* mutants, although staining in the vulval region is more extensive than that of wild-type animals. D, *srf-4(ct109)*. E, *srf-5(ct115)*. F, *srf-8(dv38)*. G, *srf-9(dv4)*. [The *srf-2*, *-3*, *-4*, *-5* and *-9* animals also contained *him-5(e1490)*.] Size bar = 150 μm.

ing gonad into the U-shaped tube found in adult hermaphrodites require proper migration of the distal tip cells (HEDGECOCK, CULOTTI and HALL 1987). Alterations in the trajectory of the migrating distal tip cells lead to predictable abnormalities in adult gonad morphology. For example, *unc-6* mutants, which are defective in circumferential migration of the distal tip cells, commonly have "ventralized" gonads (HEDGECOCK, CULOTTI and HALL 1990). We observed similar, although usually less severe, defects in adult gonad morphology in the pleiotropic *srf* mutants (see Figure 4, C and D; Table 5).

**Immunocytochemistry:** The uncoordinated movement of the pleiotropic *srf* mutants suggested that these mutants may have muscle or neuronal defects. All of the pleiotropic alleles have essentially identical uncoordinated phenotypes, characterized by slow movement, occasionally nonsinusoidal body posture, and a distinctive "head-waving" backwards movement displayed when the animals are prodded at the head. Muscle structure in these mutants was examined by polarization optics visualization of muscle birefringence and actin staining using fluorescently labeled phallacidin (FRANCIS and WATERSTON 1985). Muscle fiber organization and muscle cell arrangement appeared generally wild-type in all of the pleiotropic mutants (see Figure 5, A and B).

The pleiotropic *srf* mutants were also examined for neuronal defects. Specifically, we sought to determine if these mutants have neuronal structural defects, as has been demonstrated for *unc-6* (SIDDIQUI 1990). We were able to examine a subset of neurons using probes for the DD and VD motor neurons, and the ALM mechanosensory neurons.

The structure of the DD and VD motor neurons was visualized using anti-GABA antisera, which specifically binds to these neurons (JOHNSON and STRETTON 1987; S. MCINTIRE, personal communication). In

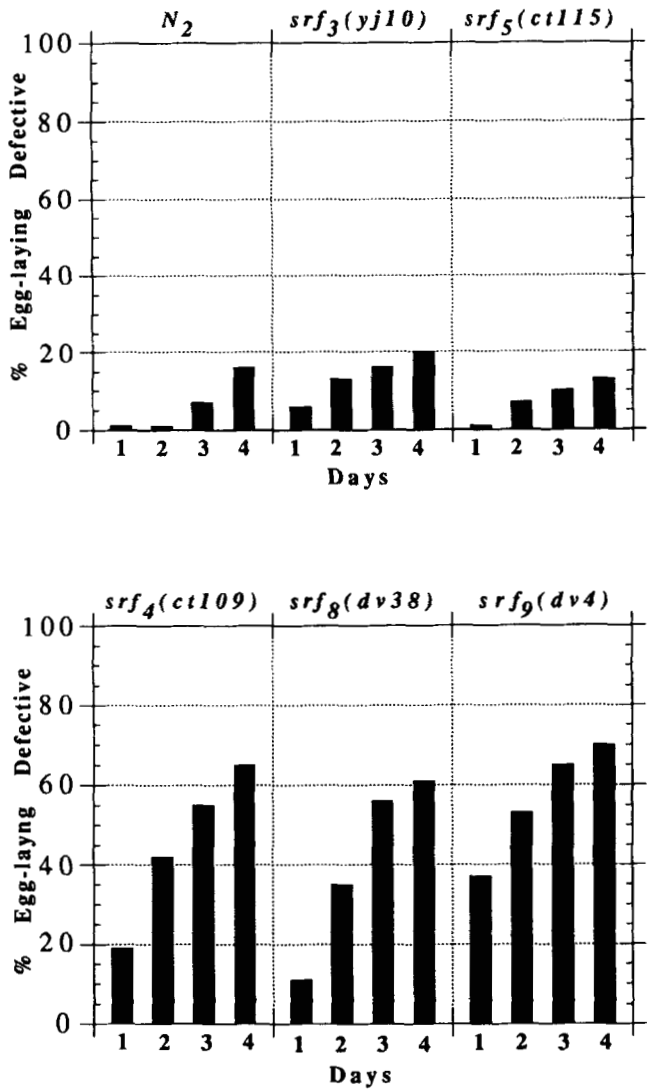


FIGURE 3.—Egg-laying in wild-type and *srf* mutant animals. Fourth larval stage hermaphrodites were individually transferred to NGM plates. After 20–24-hr incubation at 20° (day 1), animals were scored for the bloated appearance characteristic of egg-laying defective animals. These animals were rescored for this phenotype for the following 3 days (days 2, 3 and 4). The histograms represent the cumulative number of egg-laying defective animals. One hundred (or more) animals were scored for each genotype.

wild-type animals, these neurons have cell bodies in the ventral nerve cord that send projections (commissures) circumferentially to the dorsal cord (see Figure 6A). In *unc-6* mutants, these commissures are severely affected, and rarely reach the dorsal cord (see Figure 6B). In the pleiotropic *srf* mutants, these commissures reach the dorsal cord normally, although their morphology is quantitatively different from wild-type commissures (see Figure 6, C and D). As shown in Table 6, the commissures of the pleiotropic *srf* mutants have many more varicosities than those of wild-type animals, and are also more likely to cross or fasciculate with neighboring commissures. The three pleiotropic *srf* alleles examined are very similar in

**TABLE 3**

**Summary of mutant phenotypes**

| Genotype | Movement | Male bursa | Egg laying | Dauer larvae |
|---|---|---|---|---|
| *srf-2(ct104)* | + | + | + | + |
| *srf-3(ct107)* | + | + | + | SDS sens. |
| *srf-4(ct109)* | Unc | Mab | Egl | SDS sens. |
| *srf-5(ct115)* | + | + | + | + |
| *srf-8(dv38)* | Unc | Mab | Egl | SDS sens. |
| *srf-9(dv4)* | Unc | Mab | Egl | SDS sens. |

+ = indistinguishable from wild-type animals. Unc = uncoordinated movement. Mab = abnormal male bursae. Egl = egg-laying defective. SDS sens. = dauer larvae do not survive 1-hr treatment in 1% SDS.

**TABLE 4**

**Egg-laying response to serotonin and imipramine**

| Genotype | Eggs Laid per Animal | | |
|---|---|---|---|
| | M9 | Serotonin | Imipramine |
| N2 | 0.8 ± 0.4 | 9.2 ± 2.4 | 9.8 ± 3.8 |
| *srf-2(ct104)* | 0.3 ± 0.2 | 3.7 ± 1.2 | 6.8 ± 2.4 |
| *srf-3(yj10)* | 0.7 ± 0.3 | 11.9 ± 3.0 | 16.6 ± 3.6 |
| *srf-4(ct109)* | 0.4 ± 0.3 | 1.0 ± 0.7 | 1.3 ± 1.1 |
| *srf-5(ct115)* | 0.3 ± 0.3 | 2.6 ± 1.4 | 1.4 ± 0.7 |
| *srf-8(dv38)* | 0.3 ± 0.3 | 1.7 ± 0.9 | 2.8 ± 1.2 |
| *srf-9(dv4)* | 0.1 ± 0.1 | 1.2 ± 0.6 | 2.0 ± 0.9 |

For each genotype, five young adult hermaphrodites (staged from eggs) were incubated in a 35-μl drop of M9 buffer containing either 2.5 mg/ml serotonin or 7.5 mg/ml imipramine for one hour at 20°, and the total number of eggs were scored. Twenty replicates of each genotype were done for the serotonin and imipramine tests; eight replicates were done for the M9 buffer controls.

their frequencies of varicosities and crossed or fasciculated commissures.

The six mechanosensory touch cells have an unusual microtubule structure (CHALFIE and THOMSON 1982) and can be visualized using a monoclonal antibody, 6-11B-1, originally raised against acetylated tubulin (SIDDIQUI *et al.* 1989). Although these neurons are not directly involved in movement, we chose to examine them as well characterized "surrogate" neurons to ask if any neuronal morphology abnormalities could be observed in the pleiotropic *srf* mutants. Whole-mount squash preparations of wild-type and pleiotropic *srf* mutant animals were stained with antibody 6-11B-1. We restricted our observations to the two anterior lateral touch cells (ALML and ALMR), since these neurons could be unambiguously scored in squashed preparations. In wild-type animals, these cells send a single anterior projection to the nerve ring (see Figure 7A). In the pleiotropic *srf* mutants, these cells were often found to have an additional posterior projection (see Table 7, Figure 7B).

To confirm the abnormal ALM posterior projections observed in the pleiotropic *srf* mutants using the 6-11B-1 antibody, an alternative approach was used to visualize the ALM cells. This approach employed

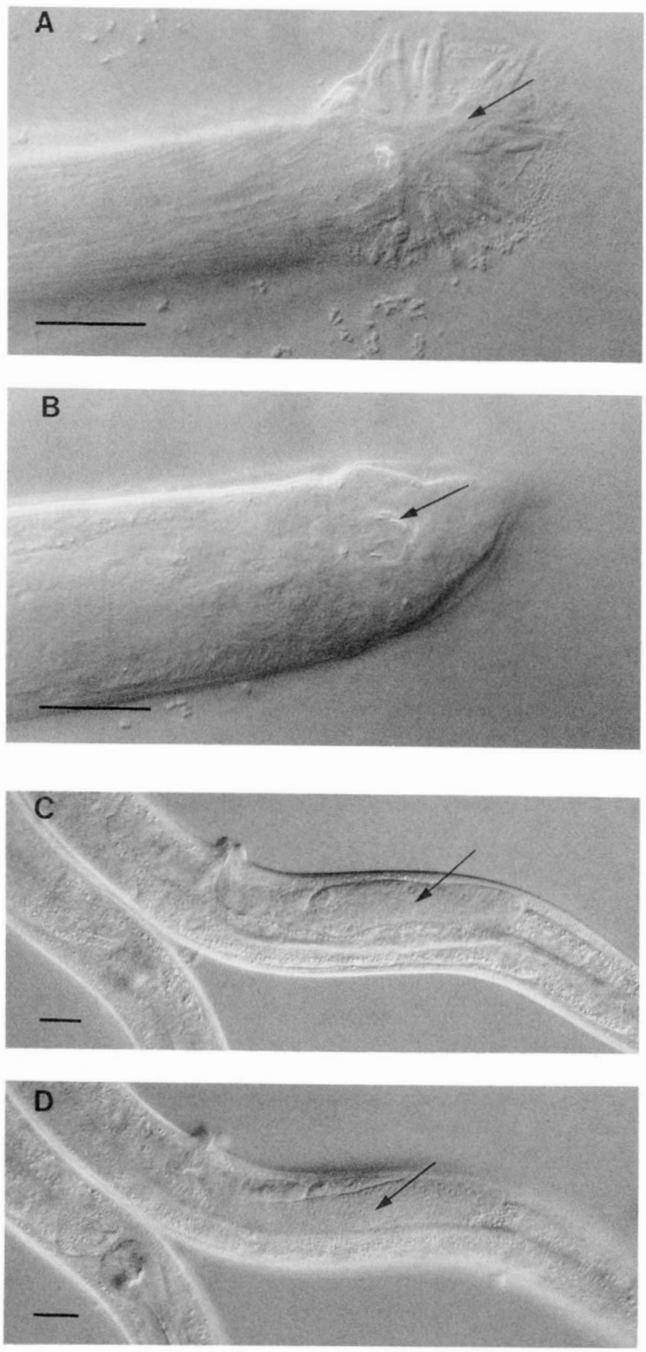


FIGURE 4.—Copulatory bursa and gonad abnormalities in *srf* mutants. Live animals were mounted on agar slabs in 0.1% sodium azide and observed under DIC optics. A, Ventral view of *him-5(e1490) srf-4(ct109)* male copulatory bursa (ventral focal plane). Note swollen bursa (arrow). [For comparable view of wild-type bursa, see LINK, EHRENFELS and WOOD (1988).] B, Same view as A, but more dorsal focal plane. Note malformed copulatory spicules (arrow). C, Young adult *srf-9(dv4) srf-8(dv38) srf-4(ct109)* hermaphrodite, focal plane through proximal portion of the posterior gonad (arrow). D, Same view as C, except focal plane through distal portion of gonad (arrow). Note that both proximal and distal sections of the gonad are located in the ventral portion of the animal, and thus the posterior gonad is lying in an abnormal left/right orientation. Size bar = 20 μm.

TABLE 5

**Gonad morphology of pleiotropic *srf* mutants**

| Genotype | Percent abnormal gonads | |
|---|---|---|
| | Anterior | Posterior |
| N2 | 0 | 0 |
| *srf-4(ct109)* | 2 | 39 |
| *srf-8(dv38)* | 8 | 59 |
| *srf-9(dv4)* | 5 | 30 |
| *srf-9(dv4) srf-8(dv38) srf-4(ct109)* | 7 | 43 |

One hundred young adult animals of each genotype were scored by DIC optics at 400×. Gonad arms were scored as abnormal if the overall morphology, particularly in the area of the gonad reflection, differed significantly from wild-type animals. The most common defect for all *srf* genotypes was the misplacement of the distal portion of the gonad to a more ventral position in the animal.

genetic constructs containing a transgenic reporter gene whose expression is restricted to the touch cells. A chimeric gene containing the *mec-7* control region fused to the *E. coli lac-Z* gene has been constructed and introduced into wild-type *C. elegans* animals by microinjection resulting in a transgenic strain that expresses β-galactosidase activity only in the touch cells (M. HAMELIN, personal communication). We introduced a chromosomally integrated copy of this transgene into the pleiotropic *srf* mutants by standard genetic techniques (see MATERIALS AND METHODS). When these animals were stained for β-galactosidase activity, ALM neurons with posterior processes were occasionally observed in the pleiotropic *srf* mutants (see Figure 7C). However, the fraction of ALM neurons observed to have posterior processes by this method was significantly smaller than the fraction determined by 6-11B-1 staining. For example, in *srf-4* transgenic animals, only 6/138 ALM neurons showed posterior processes by β-galactosidase staining, while 28/81 ALM neurons were observed to have posterior processes in *srf-4* animals stained with antibody 6-11B-1. This difference may result from the (presumably nonfunctional) posterior processes containing microtubules but being unable to accumulate β-galactosidase.

**Interactions with lin-12:** The pleiotropic *srf* mutants were observed to have a low penetrance, weakly expressive multivulval (Muv) phenotype. A much more dramatic Muv phenotype was observed when the pleiotropic *srf* mutants were combined with *lin-12(n302)*. This weak dominant *lin-12* allele (GREENWALD, STERMBERG and HORVITZ 1983) also produces a low penetrance, weak Muv phenotype. Double mutant *lin-12(n302);* pleiotropic *srf* constructs have a highly penetrant, strong Muv phenotype characteristic of strong dominant *lin-12* alleles (see Table 8). None of the nonpleiotropic *srf* mutants show this apparent enhancement of *lin-12(n302)*. This interaction does not appear to be allele-specific. For example,

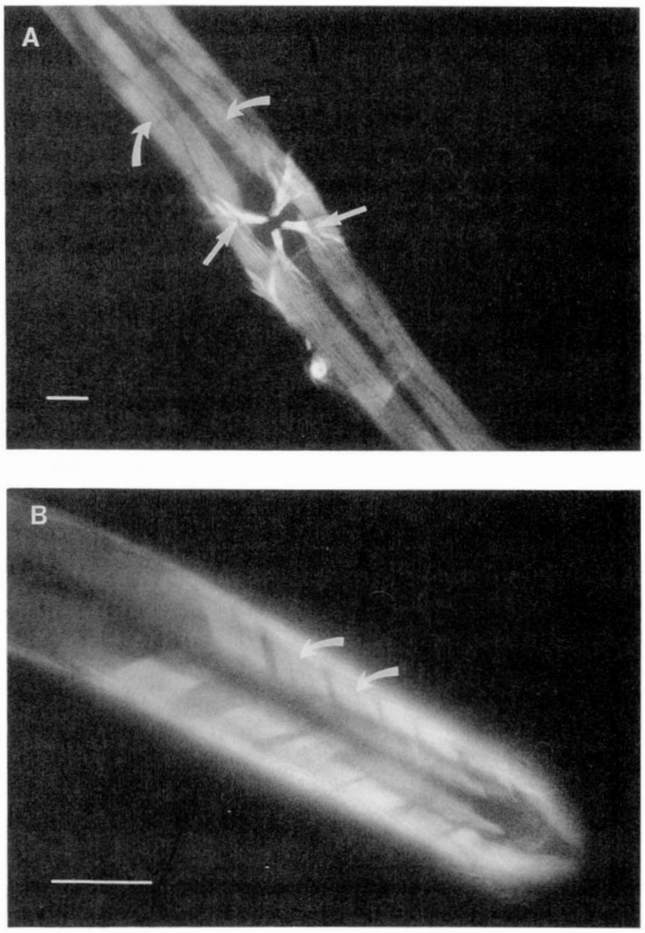


FIGURE 5.—Muscle structure in *srf-4* animals. Animals were fixed and stained with Bodipy-phallacidin as described in MATERIALS AND METHODS. A, Ventral mid-animal view of *srf-4* hermaphrodite stained with Bodipy-phallacidin. Note structure of body wall muscles (curved arrows) and vulval muscles (straight arrows). B, Ventral posterior view of *srf-4* male stained with Bodipy-phallacidin. Note normal structure of diagonal sex muscles (arrows). Size bar = 20 μm.

*srf-4(ct109)* also enhances the Muv phenotype of the weak dominant *lin-12(n379)* allele as well as the strong dominant/hypomorphic recessive allele combination *lin-12(n676n930)*. In contrast, *srf-4(ct109)* appeared to have no effect on the recessive (putative null) *lin-12* allele *n904 am*, as *lin-12(n904am); srf-4(ct109)* animals had the characteristic vulvaless phenotype seen in *lin-12(n904am)* animals (data not shown).

## DISCUSSION

We have identified six genes that can mutate to produce ectopic surface binding of the lectin WGA. Two of these genes, *srf-2* and *srf-3*, had previously been identified in a screen designed to identify larval animals expressing adult surface antigens (POLITZ *et al.* 1990). Ectopic surface binding of lectins could theoretically result from either the deposition of novel carbohydrate residues on the cuticle surface or the removal of surface components that normally mask endogenous carbohydrates. Surface radiolabeling experiments with *srf-2* and *srf-3* mutants have indicated that these mutants are missing surface proteins normally found on wild-type animals (POLITZ *et al.* 1990; M. BLAXTER, personal communication). We have performed similar surface radiolabeling experiments with representative alleles of the six *srf* genes, and found a protein of approximately 10 kD that strongly labels in wild-type animals and is missing or strongly diminished in these mutants (data not shown). These results are consistent with the recessive nature of these mutations, and suggest that the lectin-binding phenotypes caused by these mutations have similar (immediate) biochemical origins.

The *srf* mutants could be readily divided into two classes based on their additional phenotypes. Except for their lectin-binding phenotypes, *srf-2*, *srf-3* and *srf-5* mutations appear grossly wild-type, while *srf-4*, *srf-8* and *srf-9* mutants have a collection of pleiotropic effects, including uncoordinated movement, defective egg-laying, and abnormal gonad and bursal morphology. (This division of these mutants into pleiotropic and nonpleiotropic classes is imperfect, as the *srf-3* mutants also have SDS-sensitive dauer larvae. We have grouped the *srf-3* mutants in the nonpleiotropic class because of their much greater overall similarity to the *srf-2* and *srf-5* mutants.) We have focused on the pleiotropic mutants because we suspect these animals are defective in a process involved in cell-cell or cell-matrix interactions occurring in a range of developmental processes (see arguments below). The following observations suggest that the best characterized pleiotropic alleles [*srf-4(ct109)*, *srf-8(dv38)* and *srf-9(dv4)*] are likely to be strong or complete loss-of-function alleles. First, *srf-4(ct109)/Df* (*ozDf1* or *yDf4*) and *srf-9(dv4)/sDf35* animals are indistinguishable (at least by plate phenotype) from the homozygous mutants (no deficiencies are available for the *srf-8* region). Second, the 11 alleles in the pleiotropic class, despite being identified solely on the basis of their ectopic lectin binding, have very similar, complex phenotypes. This similarity of phenotypes would be unlikely if these were hypomorphic alleles. Although the incomplete penetrance of some of the pleiotropic defects might imply some residual gene function in these alleles, it is not uncommon in *C. elegans* for null alleles of genes involved in developmental processes to show incomplete penetrance [*e.g.*, animals containing *unc-6(e400)*, a presumed null allele of *unc-6*, can have normal gonads.]

Male animals containing any of the pleiotropic *srf* mutations have abnormal copulatory bursae, commonly with crumpled or misshapen spicules. The copulatory spicules are hollow, sclerotized, spikelike structures that are formed by descendents of the B blast cell (SULSTON, ALBERTSON and THOMSON 1980);

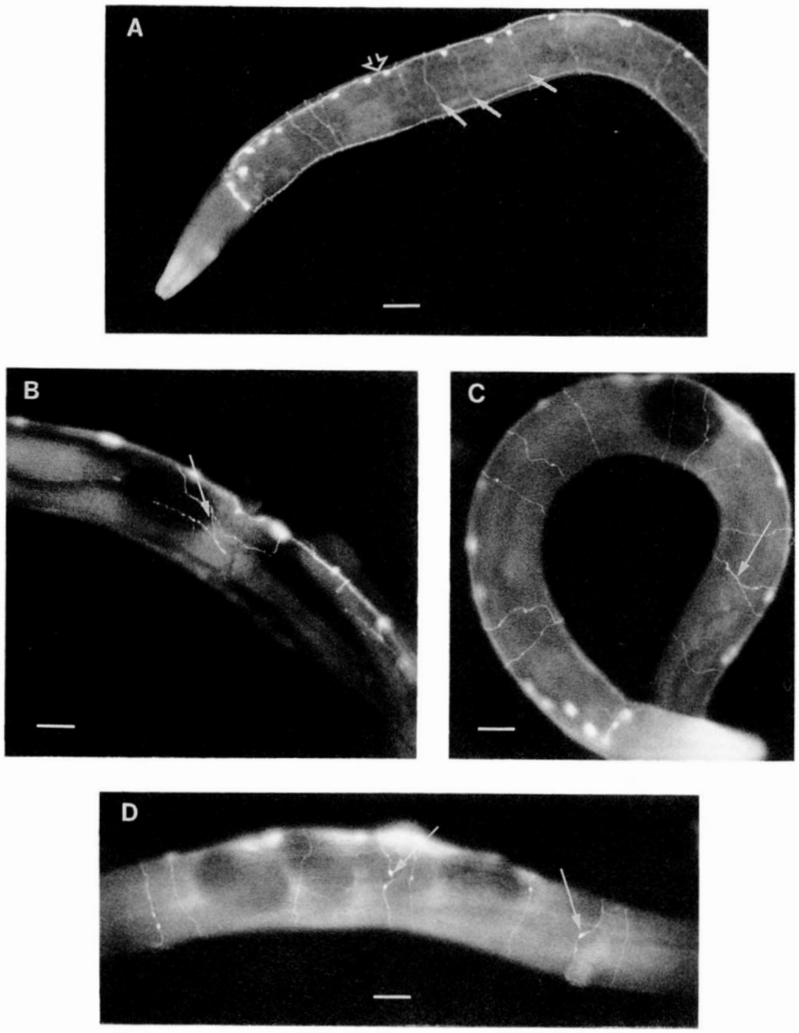


FIGURE 6.—Immunological staining of GABA-nergic neurons in wild-type and mutant animals. Animals were fixed and stained with anti-GABA antisera as described in MATERIALS AND METHODS. A, Wild-type animal. The DD and VD motor neurons have cell bodies in the ventral nerve cord (open arrow) and send circumferential processes (commissures, closed arrows) to the dorsal nerve cord. B, *unc-6* animal. Commissures fail to reach the dorsal nerve cord (arrow). C, *srf-4* animal. Commissures reach dorsal cord, but have increased frequency of crossed or fasciculated commissures (arrow). D, *srf-4* animal. Commissures have increased frequencies of varicosities (arrows). Size bar = 20 μm.

**TABLE 6**

**Quantifying DD and VD commissure morphological abnormalities**

| Strain | Animals scored | Commissures scored | Abnormal commissures | Total varicosities | Percent abnormal commissures | Varicosities/ commissure |
|---|---|---|---|---|---|---|
| N2 | 63 | 623 | 27 | 44 | 4.3 | 0.07 |
| *srf-4(ct109)* | 28 | 260 | 23 | 85 | 8.8 | 0.33 |
| *srf-8(dv38)* | 25 | 240 | 25 | 70 | 10.4 | 0.29 |
| *srf-9(dv4)* | 38 | 366 | 38 | 117 | 10.4 | 0.32 |
| *srf-9(dv4) srf-8(dv38) srf-4(ct109)* | 23 | 244 | 20 | 104 | 9.0 | 0.43 |

Animals were fixed and stained with anti-GABA antibodies as described in MATERIALS AND METHODS. Scoring was done blindly and was restricted to predominantly intact adult animals in which at least seven commissures were scorable. Commissures were scored as abnormal if they crossed or fasciculated with neighboring commissures.

mutations that perturb the B cell lineage can result in abnormal spicules. The pleiotropic *srf* mutants, however, appear to have normal B cell lineages (H. CHAMBERLIN, personal communication). Proper spicule morphogenesis also requires proper function or attachment of the male sex muscles, as well as proper secretion of the spicule material by B cell descendents. Either of these processes may be defective in the pleiotropic *srf* mutants.

The pleiotropic *srf* mutants show a progressive egg-laying defect (see Figure 3) and reduced sensitivity to exogenous serotonin and imipramine (see Table 4). This reduced sensitivity could result from non- or subfunctional vulval muscles. (As shown in Figure 5A, vulval muscles in these mutants appear to have normal morphology.) An alternative explanation is that this reduced sensitivity results because the pleiotropic *srf* mutants are less permeable to serotonin and imiprimine. We note that nonpleiotropic *srf-3* and *srf-5* animals have wild-type egg-laying but show altered serotonin and imipramine responses. (*srf-3* animals are hypersensitive to these compounds; *srf-5* animals

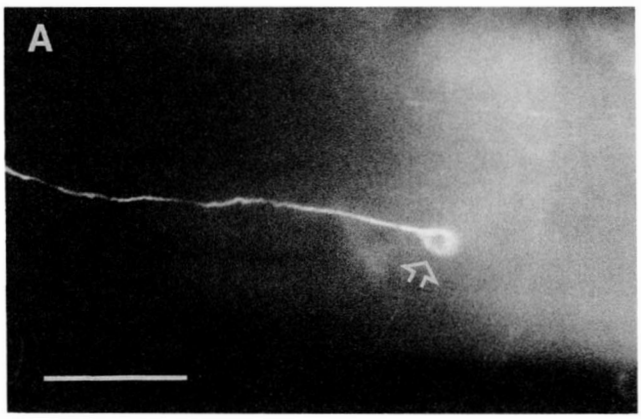


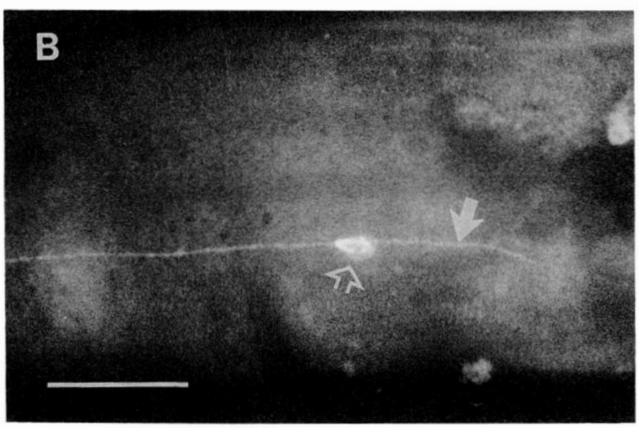


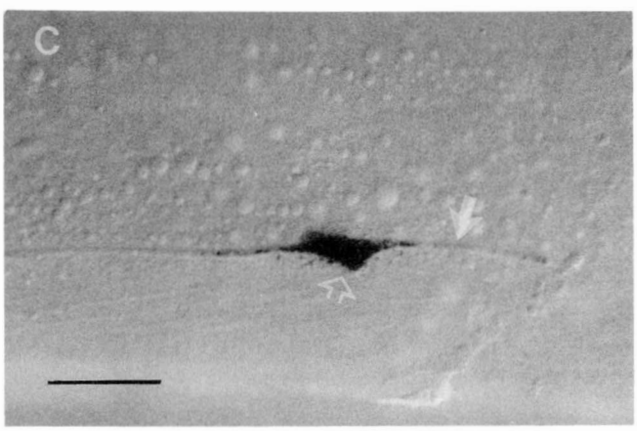


FIGURE 7.—Staining of ALM mechanosensory neurons in wild-type and mutant animals. Animals were fixed and stained as described in MATERIALS AND METHODS. A, Visualization of ALM neuron in wild-type animals using anti-acetylated tubulin antibody 6-11B-1. Note single process extending anteriorly from cell body (open arrow). B, Visualization of ALM neuron in *srf-9(dv-4)* animal using antibody 6-11B-1. Note posterior process (closed arrow) extending from cell body (open arrow). C, Visualization of ALM neuron in *srf-8(dv38)* animals containing *mec-7/lac Z* transgene by β-galactosidase staining. Note posterior process (closed arrow) extending from cell body (open arrow). Size bar = 20 μm.

show reduced sensitivity.) In light of these observations, it is difficult to interpret the serotonin and imipramine responses of the pleiotropic *srf* mutants, and the basis of the egg-laying defect in these mutants remains unclear.

**TABLE 7**

**Quantifying posterior processes in ALM neurons**

| Genotype | ALM neurons with posterior processes per total ALMs scored | Percent abnormal ALMs |
|---|---|---|
| N2 | 1/50 | 2.0 |
| *srf-4(ct109)* | 28/81 | 34.6 |
| *srf-8(dv38)* | 9/58 | 15.5 |
| *srf-9(dv4)* | 42/78 | 53.8 |
| *srf-9(dv4)srf-8(dv38)srf-4(ct109)* | 36/63 | 57.1 |

Animals were fixed and stained with antibody 6-11B-1 using the whole mount squash protocol of SIDDIQUI (1990). ALM neurons of adult hermaphrodites were scored for posteriorly-directed axonal projections by epifluorescence microscopy. ALM neurons were judged to have a posterior projection if a posteriorly directed axonal projection longer than the width of the ALM cell body was observed.

**TABLE 8**

**Multivulval (Muv) phenotypes of single and double mutants**

| Genotype | Fraction Muv | Percent Muv |
|---|---|---|
| *lin-12(n302)* | 80/654 | 12.2 |
| *srf-4(ct109)* | 34/500 | 6.8 |
| *srf-8(dv38)* | 4/502 | 0.8 |
| *srf-9(dv4)* | 12/500 | 2.4 |
| *lin-12(n302); srf-4(ct109)* | 261/262 | 99.6 |
| *lin-12(n302); srf-8(dv38)* | 104/105 | 99.0 |
| *lin-12(n302); srf-9(dv4)* | 93/95 | 97.9 |
| *lin-12(n302); srf-2(ct104)* | 11/104 | 10.6 |
| *lin-12(n302); srf-3(yj10)* | 17/100 | 17.0 |
| *lin-12(n302); srf-5(ct115)* | 16/101 | 15.8 |
| *lin-12(n379)* | 25/448 | 5.6 |
| *lin-12(n379); srf-4(ct109)* | 131/187 | 70.0 |
| *lin-12(n676 n930)* (16°) | 0/72 | 0 |
| *lin-12(n676 n930); srf-4(ct109)* | 104/105 | 99.0 |
| *lin-12(n302); srf-4(ct109)/+* | 138/458 | 30.1 |
| *glp-1(q35)* | 21/107 | 19.6 |
| *glp-1(q35); srf-4(ct109)* | 25/141 | 17.7 |

Animals were mounted on agar slabs on microscope slides with coverslips and scored with a dissecting microscope at 50×, with the exception of the *lin-12(n302)*; pleiotropic *srf* double mutants, which were scored at 400× under DIC optics. [This alternative scoring procedure was used because these animals were derived from heterozygous mothers, and were therefore stained with WGA-FITC and examined by epifluorescence microscopy to confirm their genotype. Homozygous ($WGA^+$) or heterozygous ($WGA^-$) animals were then scored by DIC optics. In these experiments, *srf-4(ct109)* was balanced with an *unc-51(e369) rol-9(sc148)* chromosome, while *srf-8(dv38)* and *srf-9(dv4)* were balanced with an *unc-68(e540) sma-1(e30)* chromosome.] Animals were scored as Muv if they were observed to have two or more vulval protrusions.

The pleiotropic *srf* mutants have variably abnormal gonad morphology, the most common defect being the ventral mispositioning of the distal portion of the gonad. We interpret these gonad abnormalities as the result of abnormal migration of the distal tip cells that lead the growing gonad. For all the *srf* mutants examined, the posterior arm of the gonad is much more likely to be abnormal; this unexplained bias has also been observed for other mutations that affect gonad morphology (HEDGECOCK, CULOTTI and HALL 1990).

Although the *srf* mutants typically have ventralized gonads, other abnormalities have been observed. For example, animals were occasionally observed to have "Z"-shaped gonads, presumably the result of the distal tip cell migrating centripetally (opposite of the normal migration) after reaching the dorsal side. [Gonads with this morphology are seen in *dpy-24* mutants (HEDGECOCK *et al.* 1987).] HEDGECOCK, CULOTTI and HALL (1990) have interpreted the ventralized gonads observed in *unc-6* mutants to be the result of a general inability of cells to migrate circumferentially. The range of gonad morphology abnormalities in the *srf* mutants suggests that these mutants may have a less specific migration defect.

The pleiotropic *srf* mutants have uncoordinated movement, but apparently normal body wall muscle structure. In these mutants, we observed specific axonal abnormalities in the subset of nerve cells that we were able to visualize using immunocytochemical staining. The DD and VD neurons had an increase in varicosities and in the fraction of crossed or fasciculated commissures, while the ALM neurons had an increased fraction of posteriorly directed processes. Neither of these defects is likely to account directly for the uncoordinated movement in these mutants, as the ALM neurons are mechanosensory, and the level of defects seen in the DD and VD neurons seems insufficient to cause the *srf* uncoordinated phenotype, which is completely penetrant and highly reproducible from animal to animal. Instead, the uncoordinated phenotype may result from structural or functional defects in other neurons that were not scored.

Our most surprising finding was the strong enhancement of weak dominant *lin-12* alleles by the pleiotropic *srf* mutations. The *lin-12* gene encodes an apparent cell surface receptor with strong homology to the Drosophila *Notch* gene (YOCHEM and GREENWALD 1989). Dominant *lin-12* alleles behave genetically as if they are constitutive or hypersensitive for receptor activation. The *srf:lin-12* interaction is unlikely to be a secondary result of the other pleiotropic defects: *srf-4(ct109)*/+ animals, which are phenotypically wild-type for all dissecting microscope phenotypes, show significant enhancement of *lin-12(n302)* (see Table 8). This point is also supported by the observation that the nonpleiotropic *srf* mutants do not significantly enhance *lin-12(n302)*, despite having lectin-binding and surface-radiolabeling characteristics similar to the pleiotropic *srf* mutants. The enhancement of *lin-12* is also not restricted to the vulval lineages. Unlike *lin-12(n302)* or *srf-4(ct109)* males, *lin-12(n302);srf-4(ct109)* males have ectopic sensory hooks, indicative of P9.p and P11.p cells assuming the P10.p cell fate, as observed in strong dominant *lin-12* alleles (data not shown).

The phenotypic similarities of *srf-4*, *srf-8* and *srf-9* alleles suggest that these genes are involved in the same biological process. One simple interpretation is that these genes function in different steps of a linear, sequential pathway, and removal of gene function at any step leads to dysfunction of the pathway. We have tested this hypothesis by constructing a *srf-4(ct109) srf-8(dv38) srf-9(dv4)* triple mutant (see MATERIALS AND METHODS). This triple mutant is indistinguishable from the single mutants under the dissecting microscope and has quantitatively similar neurological and gonadal defects (see Tables 5 and 6). This result supports the linear pathway model and argues against these genes functioning in an additive or parallel manner.

All the mutations that we have identified perturb the normal localization (or accessibility) of cuticle carbohydrates. The recessive nature of these mutations, along with surface radiolabeling experiments, suggest that the ectopic lectin binding of these mutants results from the modification or absence of a cortical cuticle layer. Since mutations in the genes *srf-2*, *srf-3* and *srf-5* result in defects apparently restricted to the cuticle, these genes may encode structural cuticle proteins or proteins required for proper cuticle assembly or modification. In contrast, mutations in *srf-4*, *srf-8* and *srf-9* genes lead to developmental defects that cannot be explained by cuticle abnormalities. What is the underlying defect in the pleiotropic *srf* mutants? In the following discussion, we address this question by considering two related issues: what is the site of pleiotropic *srf* gene action, and what are the molecular functions of these genes?

Despite the range of phenotypes observed in the pleiotropic *srf* mutants, the action of these genes may be restricted to one tissue, the hypodermis. Clearly, defects in hypodermal function could account for the cuticle alterations observed in the pleiotropic *srf* mutants, since the hypodermis secretes the cuticle. The hypodermis also plays an important role in the development of internal structures, because it secretes a basal lamina. This lamina is the site of (and possibly substrate for) distal tip cell migration, axon pathfinding, and muscle cell attachment. Thus, the neuronal and gonadal defects observed in the pleiotropic mutants could result from a defective basal lamina. This appears to be the primary defect in *unc-6* mutants, as the *unc-6* gene has been shown to encode a laminin-like molecule (W. WADSWORTH and E. M. HEDGECOCK, personal communication). An alternative hypothesis is that the pleiotropic *srf* phenotypes result from absence of gene function in multiple tissues (*i.e.*, distal tip cell migration abnormalities result from defective *srf* gene function in these cells). These competing hypotheses should be readily testable by genetic mosaic analysis using free duplications (HERMAN 1989).

The enhanced multivulval phenotype observed in *lin-12(n302)*; pleiotropic *srf* double mutants also involves hypodermal tissue, as hypodermal cells assume vulval cell fates. This enhancement may act either cell autonomously (*i.e.*, requiring the absence of *srf* gene function in the cells assuming the vulval cell fate), or non-cell autonomously. Pleiotropic *srf* mutations could enhance weak *lin-12* dominant mutants by altering the makeup or amount of the *lin-12* receptor protein, such that its level of activation is effectively increased. Alternatively, pleiotropic *srf* mutations could act downstream of the *lin-12* receptor in an intracellular signalling system to increase the activation of the vulval cell fate. These two models would predict cell autonomous enhancement. Other models posit that pleiotropic *srf* mutations promote *lin-12* activation by increasing the effective concentration of the (currently unidentified) *lin-12* ligand. In these models, *lin-12* enhancement could occur in a non-cell autonomous manner.

The interaction between *lin-12* and pleiotropic *srf* mutations is reminiscent of the interaction of *glp-1* and *dumpy* (*dpy*) mutations (MAINE and KIMBLE 1989). *glp-1* mutations perturb germline proliferation (AUSTIN and KIMBLE 1987) and embryonic induction of the pharynx (PRIESS, SCHNABEL and SCHNABEL 1987). This gene encodes a putative receptor protein with homology to *lin-12* (YOCHEM, WESTON and GREENWALD 1988); *glp-1* and *lin-12* have also been shown to have overlapping functions (LAMBIE and KIMBLE 1991). Hypomorphic recessive alleles of *glp-1* can be suppressed by recessive mutations in *dpy-1*, *-2*, *-3*, *-7*, *-8*, *-9*, *-10* and *sqt-1*. These suppressing mutations all cause altered body shape; *sqt-1* has been shown to encode a collagen gene (KRAMER *et al.* 1988). It has been proposed that the *glp-1* suppression occurs via changes in the extracellular matrix (MAINE and KIMBLE 1989). Similar arguments can be made for the mechanism of *srf* enhancement of *lin-12*, implying a potentially non-cell autonomous interaction.

The *glp-1: dpy* and *lin-12: srf* interactions differ in a number of respects, however. Although both interactions may result from an effective increase in gene function, the *dpy* mutations suppress recessive *glp-1* alleles, while the *srf* mutations enhance dominant *lin-12* alleles. (To our knowledge, no *glp-1* alleles dominant for the Glp phenotype or simple hypomorphic *lin-12* alleles have been identified.) We find that *srf-4(ct109)* can enhance *lin-12(n302)* in a semidominant fashion, an effect not observed between *glp-1* and *dpy-10* (MAINE and KIMBLE 1989). We have also looked for an interaction between *glp-1* and *srf-4*, but have not observed any suppression of the embryonic lethality of the hypomorphic *glp-1* alleles *e2141ts* or *e2144ts*, nor any enhancement of the weak Muv phenotype displayed by the unusual semi-dominant *glp-1* allele *q35* (see Table 8).

The broad effects of pleiotropic *srf* mutations are more readily explicable if we postulate that these mutations perturb a process, as opposed to the function of a single protein. This interpretation is consistent with the evidence that these genes function in a linear pathway instead of in a parallel, additive manner. An obvious candidate process is the modification or secretion of extracellular proteins. A defect in proper production of extracellular proteins could account for cuticle, basal lamina, and spicule abnormalities, as well as perturbations in the *lin-12* signalling system (by affecting *lin-12* receptor or ligand activities). Defects in protein secretion could occur at a biochemical level (*e.g.*, processing of signal sequences, glycosylation) or at the level of cell function (*e.g.*, proper Golgi body formation). Defects in the latter class may be discernable by ultrastructural analysis. However, because complete disruption of secretory processes would likely be lethal, we would postulate that the pleiotropic *srf* genes are required for secretion of only a subset of extracellular proteins, or, alternatively, for only some fraction of the secretion of many proteins.

If the pleiotropic *srf* mutations are defective in the processing or secretion of extracellular proteins, an underlying defect in protein glycosylation is an intriguing possibility. A block in the latter stages of glycosylation (*e.g.*, addition of terminal sugars) would seem most likely, since this would presumably affect a subset of glycoproteins. The ectopic binding of the lectins WGA and SBA (which show affinity for *N*-acetyl glucosamine and *N*-acetyl galactosamine, respectively) could conceivably result from the absence of terminal sugar residues that normally block these lectins from binding to cuticle glycoproteins. This effect has been observed in CHO cell glycosylation mutants (STANLEY 1984). There is also some experimental evidence that glycosylation can play a role in neurite outgrowth (LANDMESSER *et al.* 1990; CHANDRASEKARAN *et al.* 1991) and cell migration (BRANDLEY, SHAPER and SCHNAAR 1990; KUNEMUND *et al.* 1988; STOOLMAN 1989). It has been proposed that activation of the *lin-12* receptor gene involves multimerization of the receptor protein (GREENWALD and SEYDOUX 1990), as has been described for the insulin receptor. It is not difficult to imagine this multimerization being modulated by levels of *lin-12* protein glycosylation, thus suggesting a mechanism by which the pleiotropic *srf* mutation could alter *lin-12* function. Examination of the glycosylation hypothesis will require analysis of cuticle and basal lamina glycoproteins.

Determination of the exact function of the pleiotropic *srf* genes will likely require their molecular

cloning and sequencing. The *srf-8* and *srf-9* genes are located in a region of LGV that is completely covered by the *C. elegans* physical map (COULSON *et al.* 1986), and should be recoverable by positional cloning approaches (*e.g.*, HAN and STERNBERG 1990).

We would like to thank H. CHAMBERLIN, J. MANSER and T. BOGAERT for expert opinions on the phenotypes of our mutants; S. POLITZ and M. BLAXTER for advice on surface-labeling experiments, G. PIPERNO for providing antibody 6-11B-1; M. HAMELIN and J. WAY for providing *jeIn1*; S. SIDDIQUI, S. SALSER and L. BLOOM for advice on staining protocols; and T. SCHEDL for providing deficiency strains and genetic data. We would also like to thank C. TRENT and C. HUNTER for critical reading of this manuscript and M. ENYEART for help in its preparation. C.D.L. would like to thank W. B. WOOD, in whose laboratory this work was initiated. Some nematode strains used in this work were provided by the Caenorhabditis Genetics Center, which is funded by National Institutes of Health National Center for Research Resources (NCRR). This work was supported by National Institutes of Health grant R29 HD26087.

## LITERATURE CITED

AUSTIN, J., and J. KIMBLE, 1987 *glp-1* is required in the germ line for regulation of the decision between mitosis and meiosis in *C. elegans*. Cell **51:** 589–599.

BACIC, A., I. KAHANE and B. M. ZUCKERMAN, 1990 *Panagrellus redivivus* and *Caenorhabditis elegans*: evidence for the absence of sialic acids. Exp. Parasitol. **71:** 483–488.

BRANDLEY, B. K., J. H. SHAPER and R. L. SCHNAAR, 1990 Tumor cell haptotaxis on immobilized *N*-acetylglucosamine gradients. Dev. Biol. **140:** 161–171.

BRENNER, S., 1974 The genetics of *C. elegans*. Genetics **77:** 71–94.

CHALFIE, M., and J. N. THOMSON, 1982 Structural and functional diversity in the neuronal microtubules of *C. elegans*. J. Cell Biol. **93:** 15–23.

CHANDRASEKARAN, S., J. W. DEAN III, M. S. GINIGER and M. L. TANZER, 1991 Laminin carbohydrates are implicated in cell signaling. J. Cell. Biochem. **46:** 115–124.

COULSON, A., J. SULSTON, S. BRENNER and J. KARN, 1986 Toward a physical map of the genome of the nematode *C. elegans*. Proc. Natl. Acad. Sci. USA **83:** 7821–7825.

COX, G. N., M. KUSCH and R. S. EDGAR, 1981 The cuticle of *C. elegans*: its isolation and partial characterization. J. Cell Biol. **90:** 7–17.

COX, G. N., S. STAPRANS and R. S. EDGAR, 1981 The cuticle of *C. elegans*. II. Stage-specific changes in ultrastructure and protein composition during postembryonic development. Dev. Biol. **86:** 456–470.

DESAI, C., G. GARRIGA, S. L. MCINTIRE and H. R. HORVITZ, 1988 A genetic pathway for the development of the *Caenorhabditis elegans* HSN motor neurons. Nature **336:** 638–646.

FINNEY, M., and G. RUVKUN, 1990 The *unc-86* gene product couples cell lineage and cell identity in *C. elegans*. Cell **63:** 895–905.

FIRE, A., 1986 Integrative transformation of *C. elegans*. EMBO J. **5:** 2673–2680.

FRANCIS, G. R., and R. H. WATERSTON, 1985 Muscle organization in *C. elegans*: localization of proteins implicated in thin filament attachment and I-band organization. J. Cell Biol. **101:** 1532–1549.

GREENWALD, H. S., P. W. STERNBERG and H. R. HORVITZ, 1983 The *lin-12* locus specifies cell fates in *C. elegans*. Cell **34:** 435–444.

GREENWALD, I., and G. SEYDOUX, 1990 Analysis of gain-of-function mutations of the *lin-12* gene of *Caenorhabditis elegans*. Nature **346:** 197–199.

HAN, M., and P. W. STERNBERG, 1990 *let-60*, a gene that specifies cell fates during *C. elegans* vulval induction, encodes a *ras* protein. Cell **63:** 921–931.

HEDGECOCK, E. M., J. G. CULOTTI and D. H. HALL, 1990 The *unc-5, unc- 6*, and *unc-40* genes guide circumferential migrations of pioneer axons and mesodermal cells on the epidermis in *C. elegans*. Neuron **2:** 61–85.

HEDGECOCK, E. M., J. G. CULLOTTI, D. H. HALL and B. D. STERN, 1987 Genetics of cell and axon migrations in *C. elegans*. Development **100:** 365–382.

HERMAN, R. K., 1989 Mosaic analysis in the nematode *Caenorhabditis elegans*. J. Neurogenet. **5:** 1–24.

HODGKIN, J. A., and S. BRENNER, 1977 Mutations causing transformation of sexual phenotype in the nematode *C. elegans*. Genetics **86:** 275–287.

HODGKIN, J. A., H. R. HORVITZ and S. BRENNER, 1979 Nondisjunction mutants of the nematode *C. elegans*. Genetics **91:** 67–94.

HORVITZ, H. R., S. BRENNER, J. HODGKIN and R. K. HERMAN, 1979 A uniform genetic nomenclature for the nematode *C. elegans*. Mol. Gen. Genet. **175:** 129–133.

HORVITZ, H. R., P. W. STERNBERG, I. S. GREENWALD, W. FIXSEN and H. M. ELLIS, 1983 Mutations that affect neural cell lineages and cell fates during the development of the nematode *C. elegans*. Cold Springs Harbor Symp. Quant. Biol. **48:** 453–463.

JOHNSON, C. D., and A. O. W. STRETTON, 1987 GABA- immunoreactivity in inhibitory motor neurons of the nematode *Ascaris*. J. Neurosci. **7:** 223–235.

KEMPHUES, K. J., J. R. PRIESS, D. G. MORTON and N. CHENG, 1988 Identification of genes required for cytoplasmic localization in early *C. elegans* embryos. Cell **52:** 311–320.

KENYON, C., 1986 A gene involved in the development of the posterior body region of *C. elegans*. Cell **46:** 477–487.

KIMBLE, J., and D. HIRSH, 1979 Post-embryonic cell lineages of the hermaphrodite and male gonads in *C. elegans*. Dev. Biol. **70:** 396–417.

KRAMER, J. M., J. J. JOHNSON, R. S. EDGAR, C. BASCH and S. ROBERTS, 1988 The *sqt-1* gene of *C. elegans* encodes a collagen critical for organismal morphogenesis. Cell **55:** 555–565.

KUNEMUND, V., F. B. JUNGALWALA, G. FISCHER, D. K. H. CHOU, G. KEILHAUER and M. SCHACHNER, 1988 The L2/HNK-1 carbohydrate of neural cell adhesion molecules is involved in cell interactions. J. Cell Biol. **106:** 213–223.

LAMBIE, E. J., and J. KIMBLE, 1991 Two homologous regulatory genes, *lin-12* and *glp-1*, have overlapping functions. Development **112:** 231–240.

LANDMESSER, L., L. DAHM, J. TANG and U. RUTISHAUSER, 1990 Polysialic acid as a regulator of intramuscular nerve branching during embryonic development. Neuron **4:** 655–667.

LINK, C. D., C. W. EHRENFELS and W. B. WOOD, 1988 Mutant expression of male copulatory bursa surface markers in *Caenorhabditis elegans*. Development **103:** 485–495.

MAINE, E. M., and J. KIMBLE, 1989 Identification of genes that interact with *glp-1*, a gene required for inductive cell interactions in *Caenorhabditis elegans*. Development **105:** 133–143.

MAIZELS, R. M., W. F. GREGORY, G. E. KWAN-LOM and M. E. SELKIRK, 1989 Filarial surface antigens: the major 29 kilodalton glycoprotein and a novel 17–200 kilodalton complex from adult *Brugia malayi* parasites. Mol. Biochem. Parasitol. **32:** 213–228.

MANSER, J., and W. B. WOOD, 1990 Mutations affecting embryonic cell migrations in *Caenorhabditis elegans*. Dev. Genet. **11:** 49–64.

MCKIM, K. S., M. F. P. HESHL and D. L. BAILLIE, 1988 Genetic

organization of the *unc-60* region in *Caenorhabditis elegans*. Genetics **118:** 49–59.

POLITZ, S. M., M. PHILIPP, M. ESTEVEZ, P. J. O'BRIEN and K. J. CHIN, 1990 Genes that can be mutated to unmask hidden antigenic determinants in the cuticle of the nematode *Caenorhabditis elegans*. Proc. Natl. Acad. Sci. USA **87:** 2901–2905.

PRIESS, J. R., H. SCHNABEL and R. SCHNABEL, 1987 The *glp-1* locus and cellular interactions in early *C. elegans* embryos. Cell **51:** 601- 611.

RIDDLE, D. L., M. M. SWANSON and P. S. ALBERT, 1981 Interacting genes in nematode dauer larva formation. Nature **290:** 668–671.

ROSENBLUTH, R. E., and D. L. BAILLIE, 1981 The genetic analysis of a reciprocal translocation, eT1(II), in *C. elegans*. Genetics **99:** 415–428.

ROSENBLUTH, R. E., C. CUDDEFORD and D. L. BAILLIE, 1985 Mutagenesis in *Caenorhabditis elegans*. II. A spectrum of mutational events induced with 1500 R of gamma-radiation. Genetics **109:** 493–511.

RUDIN, W., 1990 Comparison of the cuticular structure of parasitic nematodes recognized by immunocytochemical and lectin binding studies. Acta Trop. **47:** 255–268.

SANFORD, T., M. GOLOMB and D. L. RIDDLE, 1983 RNA polymerase II from wild type and alpha-amanitin-resistant strains of *C. elegans*. J. Biol. Chem. **258:** 12804–12809.

SCHEDL, T., and J. KIMBLE, 1988 *fog-2*, a germ-line-specific sex determination gene required for hermaphrodite spermatogenesis in *C. elegans*. Genetics **119:** 43–61.

SELKIRK, M. E., W. F. GREGORY, M. YAZDANBAKHSH, R. E. JENKINS and R. E. MAIZELS, 1990 Cuticular localisation and turnover of the major surface glycoprotein (gp29) of adult *Brugia malayi*. Mol. Biochem. Parasitol. **42:** 31–44.

SIDDIQUI, S. S., 1990 Mutations affecting axonal growth and guidance of motor neurons and mechanosensory neurons in the nematode *Caenorhabditis elegans*. Neurosci. Res. **13:** 171–190.

SIDDIQUI, S. S., E. AAMODT, F. RASTINEJAD and J. CULOTTI, 1989 Anti-tubulin monoclonal antibodies that bind to specific neurons in *Caenorhabditis elegans*. J. Neurosci. **9:** 2963- 2972.

STANLEY, P., 1984 Glycosylation mutants of animal cells. Annu. Rev. Genet. **18:** 525–552.

STOOLMAN, L. M., 1989 Adhesion molecules controlling lymphocyte migration. Cell **56:** 907–910.

SULSTON, J. E., D. G. ALBERTSON and J. N. THOMSON, 1980 The *C. elegans* male: postembryonic development of nongonadal structures. Dev. Biol. **78:** 542–576

SULSTON, J. E., E. SCHIERENBERG, J. G. WHITE and J. N. THOMSON, 1983 The embryonic cell lineage of the nematode *C. elegans*. Dev. Biol. **100:** 64–119.

TRENT, C., N. TSUNG and H. R. HORVITZ, 1983 Egg-laying defective mutants of the nematode *Caenorhabditis elegans*. Genetics **104:** 619–647.

TRENT, C., W. B. WOOD and H. R. HORVITZ, 1988 A novel dominant transformer allele of the sex-determining gene *her-1* of *Caenorhabditis elegans*. Genetics **120:** 145–157.

WHITE, J. G., E. SOUTHGATE, J. N. THOMSON and S. BRENNER, 1986 The structure of the nervous system of the nematode *C. elegans*. Phil. Trans. R. Soc. Lond. **314B:** 1–340.

YOCHEM, J., and I. GREENWALD, 1989 *glp-1* and *lin-12*, genes implicated in distinct cell-cell interactions in *C. elegans*, encode similar transmembrane proteins. Cell **58:** 553–563.

YOCHEM, J., K. WESTON and I. GREENWALD, 1988 The *Caenorhabditis elegans lin-12* gene encodes a transmembrane protein with overall similarity to *Drosophila Notch*. Nature **335:** 547–550.

ZUCKERMAN, B. M., I. KAHANE and S. HIMMELHOCH, 1979 *Caenorhabditis briggsae* and *C. elegans*: partial characterization of cuticle surface carbohydrates. Exp. Parasitol. **47:** 419–424.

Communicating editor: R. K. HERMAN